SPH Simulation of Onshore Bores with Counter Rotational Vortical Structures

Maurizio LANDRINI[a], Andrea COLAGROSSI[a], Marilena GRECO[a] & Marshall P. TULIN[b]

[a] INSEAN, The Italian Ship Model Basin, Via di Vallerano 139, 00128 ROMA, Italy, a.colagrossi@insean.it

[b] Ocean Engineering Laboratory, UCSB, 6740 Cortona Drive, 93117 Goleta (CA), mpt6@cox.net

ABSTRACT

The generation and evolution of two-dimensional bores are analyzed numerically by using the Smoothed Particle Hydrodynamics (SPH) method. With this tool the bore steepening, breaking and post-breaking phases have been detailed investigated in the cases of constant and variable water depths. The bores were generated through a piston wavemaker moving with constant speed and the flow features have been studied by varying the water-depth Froude number from 0·5 to 0·95. The breaking of a plunging bore on the underlying water injects a cyclic process of splashes up with different strengths. The analysis highlighted also the occurrence of clockwise and anti-clockwise vortices, later pairing to form dipole structures. These affect the water evolution and can interact in a complex way with the free surface and with the sea floor. In the latter case, large stresses can be induced at the bottom that are responsible for instance for erosion.

INTRODUCTION

Breaking waves can release a large amount of energy in the near-shore environment that results in a turbulent flow within the water of the surf zone. This can lead to breaking rocks apart, or picking up preexisting sediment grains and tossing them about, therefore to erosion both of rocky shoreline or along a sandy beach. These and other practical consequences of near-shore breaking bores phenomena motivate an increasing research effort in this field. Not strangely, this problem and that of breaking waves approaching a sloping beach are largely discussed in the experimental literature, *e.g.* [1], [2] and [3]. However, it has been apparent for some time that new numerical approaches are necessary if we are to gain understanding and to simulate processes in water waves after the jet splashes down, throughout the post-breaking phase in the case of deep water waves, and continually throughout the cyclical splashing phase characteristic of bores. The topological origin of the vortical structures and the short time scale involved in leave to fluid viscosity a rather limited role [4].

The numerical simulation of breaking waves and post-breaking phenomena challenged several authors. The analysis of breaking bores represents a natural problem to attack early because of the richness of the fluid dynamics involved and the vigor of its splashing processes. Great advances have taken place in simulation of water wave propagation by boundary element methods up through the formation of a plunging breaker, *e.g.* [5]. Recently, some authors have simulated the post-preaking processes through more sophisticated numerical models, including the effect of a sloping beach and even turbulence models, *e.g.* [6], [7]; nonetheless, presenting only rather short evolutions. Conversely, the present investigation has permitted to evidence the cyclic post-breaking phenomena on long-time simulations. We discuss results for bores propagating on water of uniform depth, and running up along beaches with constant slope. The effects of some parameters, such as the velocity of the bore front or the steepness of the sloping beach, have also been studied. The present attempt is based on a Lagrangian method called Smoothed Particle Hydrodynamics (SPH, see *e.g.* [8] and [9]) which does not require any computational grid, and therefore is well suitable to handle free-surface breaking. In the method, the fluid is decomposed into a large number of particles, each carrying physical primitive information (density and velocity), and interacting with neighboring particles according to evolution equations which follow by discretizing the field equations for an inviscid fluid. The SPH formulation used in the present paper is detailed in [9] and [10].

BREAKING BORES

We first study the genesis and the propagation of breaking bores over water with uniform depth. The problem is sketched in Fig. 1: the flow starts with a semi-infinite layer of fluid of depth h_0, forced into motion by a vertical piston moving from left to right with constant speed U. In the discussion and in figures non-dimensional quantities are used by taking h_0 and $\sqrt{h_0/g}$ as length and time scales, respectively. In the following, we are interested in describing surface breaking and we consider the range $0{\cdot}5 \leq U/\sqrt{gh_0} \leq 0{\cdot}95$, for which the wave front steepens rapidly, overturns, and evolves into a breaking bore.

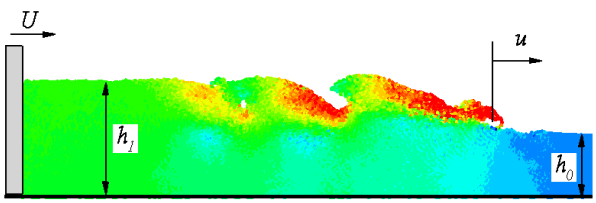

Figure 1: Sketch of a fully developed breaking bore, generated by a piston moving horizontally with velocity U in a layer of fluid with initial depth h_0. Colors represent the intensity of the velocity field.

For the fully-developed bores, after a long enough evolution, the global pattern is characterized by a breaking front moving with constant velocity, separating two layers of water with mean levels h_0 and h_1, downstream and upstream respectively. In this condition, by using the mass and momentum conservations, the dimensionless velocity of the bore $u_{\rm th}$ can be related to the water depths,

$$F_0^2 = \left(\frac{u_{\rm th}}{\sqrt{gh_0}}\right)^2 = \frac{1}{2}\left(\frac{h_1}{h_0}\right)\left(1+\frac{h_1}{h_0}\right) \ . \qquad (1)$$

During all the simulations (it occurs also in laboratory experiments), the front of the bore is not sharply defined. However, we found that, after an initial transient, the averaged velocity of the front is constant. The data from our gridless simulations are collected in Table 1, they compare very nicely with theoretical prediction (1), which is also the case of experiments [11]. This good agreement confirms that the simple momentum balance adopted in (1) is valid even though strong mixing of the surface water occurs when passing through the bore front. The vortical structures forming the wake then created actually contain considerable kinetic energy, in fluctuations, but they are rapidly convected away.

$U/\sqrt{gh_0}$	h_1/h_0	F_0	$u_{\rm SPH}/u_{\rm th}$
0·95	2·12	1·82	1·06
0·90	2·1	1·80	1·00
0·80	1·9	1·66	0·94
0·70	1·8	1·59	1·00
0·60	1·7	1·52	0·98
0·50	1·5	1·37	1·02

Table 1: Comparison between the computed velocity, $u_{\rm SPH}$, of the bore front and the theoretical value, $u_{\rm th}$, predicted by using global mass and momentum conservations, *cf.* Eq. (1).

Pre-breaking stage

We now take into consideration the case where the piston velocity is $U/\sqrt{gh_0} = 0{\cdot}8$. After the piling up of the water against the piston, a long wave starts to propagate with velocity of order $\sqrt{gh_0}$ and soon steepens, overturns and breaks with a large plunging jet impacting onto the underlying free surface. The comparison of the SPH to a BEM solver [12] is very satisfactory up to when the plunger impacts (*i.e.* when the BEM stops), *cf.* figure 2.

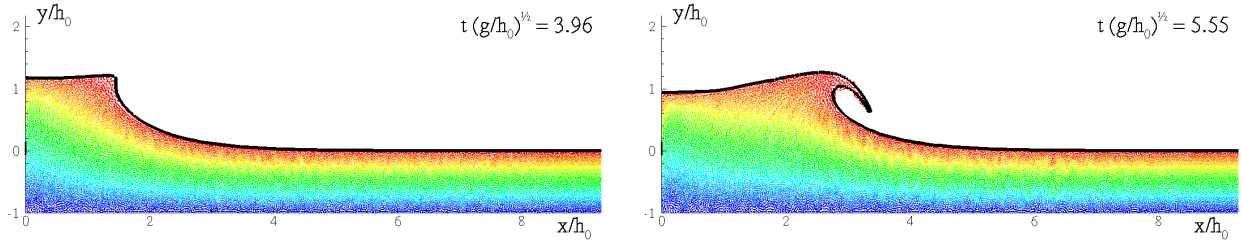

Figure 2: Pre-breaking evolution generated by a piston of constant velocity $U/\sqrt{gh_0} = 0{\cdot}8$. The coordinate system moves with the piston. Comparison of the SPH fluid domain (particles are colored according to their initial vertical height) to the BEM free-surface profiles (black solid lines).

Impact and ricochet of the plunging jet

Then, the breaking bore features repeated plunging events, which is also typical of breaking in shallow water, as in the case of wave trains approaching a beach. A detailed description of the first plunging event is instructive, also for deep-water breaking waves, and is given through the plots of Fig. 3. In particular, we have chosen for reference the configuration in the top plot, and we have assumed that the jet is formed by those particles within the area delimited by the free surface and the vertical line tangent to the nascent loop beneath the jet. These particles are colored in black. In the following plots the motion of these particles is easily tracked, thanks to the Lagrangian character of the SPH. During the free-falling phase, because of mass conservation, the jet is stretched and reduced in thickness. At the impact, the jet particles flow into two separated streams, second plot. One is deflected inside the loop, and the other one contributes to the formation of the splash-up. Up to this point, the plunger is still fed only by fresh particles (colored in red) which undergo the same evolution as the black particles. At later stages, the particles earlier entrapped by the clockwise structure, complete one revolution and (partly) re-contribute to the impinging jet, last plot, implying a strong mechanical mixing.

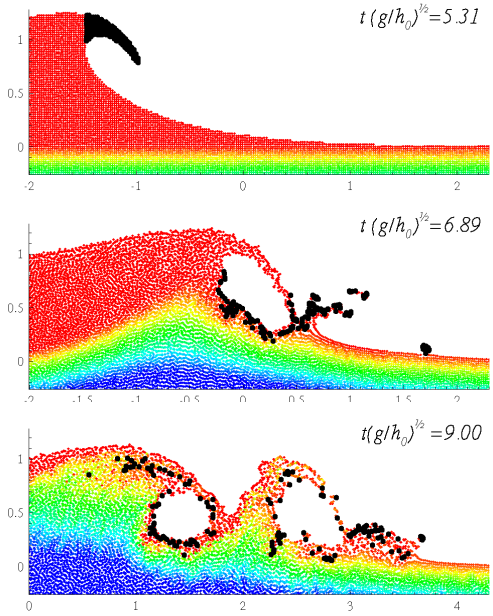

Figure 3: Evolution of the particles originally forming the plunging jet (colored in black).

Splash-up cycles and formation of vortical structures

The post-breaking evolution is described in Fig. 4. At first, attention is focused on the splash-up cycles and on the related genesis of vortical structures. In the first plot, after the impact of the plunging jet, the closure of the cavity gives rise to a clockwise-rotating structure. The impinging jet is also feeding the splash-up I, which grows in the form of a mushroom-like upwelling structure, second plot. This mushroom structure generates forward a second plunging event, giving rise to a second clockwise rotating structure, third plot. Simultaneously the other part of the mushroom structure forms a backward facing jet. The formation of this mushroom-like structure, and the growth of the backward jet, are essentially related to the gravitational collapse of the mass of water which, deflected upwards by the impact, eventually falls down, second and third plots. The further evolution of the backward-facing jet, impacting with the free surface, results in a counter-clockwise vortex, which pairs with the first one, giving origin to a peculiar flow evolution under the free surface: a dipole-like structure is formed falling down and reaching the sea floor, fourth

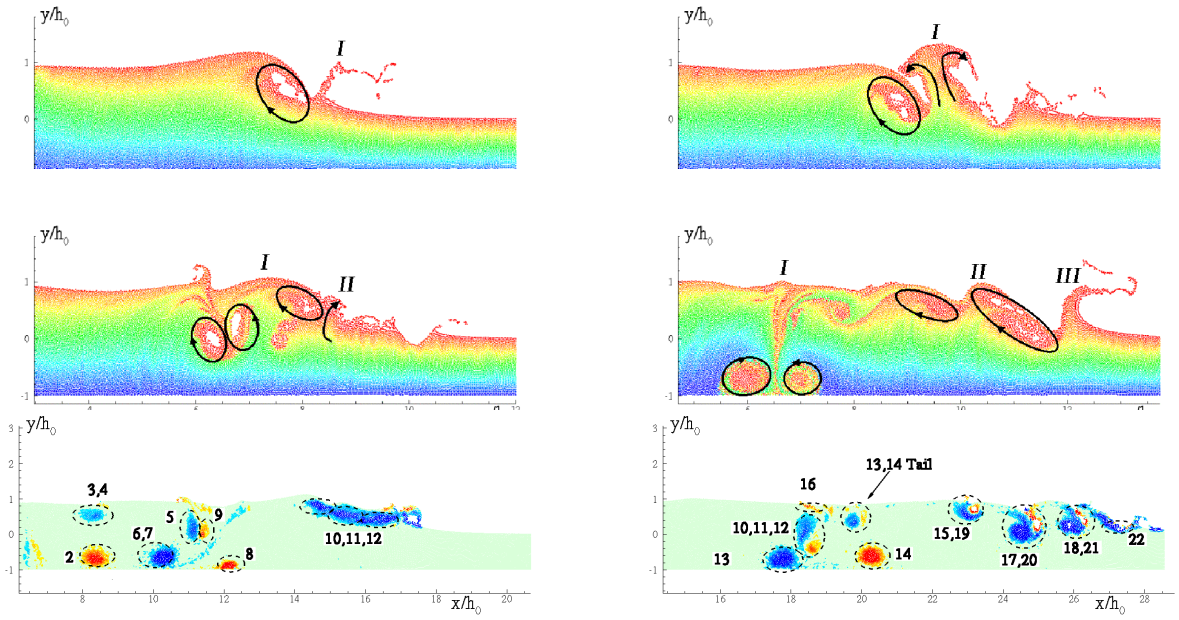

Figure 4: Further evolution of the case presented in Fig. 2 and Fig. 3. Tracking of vortical structures generated during the splash-up cycles. The non-dimensional times are $t(g/h_0)^{1/2} = 7{\cdot}92$, $10{\cdot}2$, $11{\cdot}4$, $14{\cdot}6$, $20{\cdot}7$, and $31{\cdot}5$, respectively.

plot. The strength of the backward jet governs the interaction with the free surface and therefore the features and the evolution of the resulting dipole-like structures. The second plunging breaker causes the growth of the splash-up *II* in third plot, this splash-up is less vigorous: the forward jet is rather weak and the backward flow originates later. Due to this, the formation of the counter-clockwise structures is delayed and the clockwise vortices stay longer at the free surface. Later, fourth plot in Fig. 4, a third rather energetic splash-up (*III*) originates, with similar strength of the splash-up *I*. The subsequent dipole-like structure is quite strong and falls down; and so on.

The genesis of each vortical region is related to a folding over the surface that creates a doubly connected region. This is crucial for the generation of vorticity and circulation. The described interaction phenomena resemble the experimental observations analyzed in [3] (1989, *cf.* Figs. 19 and 20) for breaking surface waves in deep water. When dipole-like structures are formed, air and surface water are captured inside and convected downwards. In the numerics the air is not modeled, but the entrapped air could affect the motion of the vortices. In this context, an important aspect to be speculated is related to the buoyancy effects due to the entrapped bubbly phase on the downward motion of the dipole structures. SPH can deal with a fluid of varying density, although the accurate estimation of the actual local variation in the fluid density is rather challenging [9]. Further, in this work we analyze only two-dimensional flows; in reality, three-dimensional effects will play a role both in the air cavity and in the vortical-structure evolutions [13].

It is not straightforward how to correlate the unsteadiness of the flow field for different speeds of the forcing piston. The approach we have taken is to count the frequency of creation of the forward splashes. Except when the backward splash is very weak, these tend to pair with backward splashes creating dipole-like structures. During their evolution the dipole structures tend to interact with each other. In the two lower plots of figure 4, the rotational areas are identified by the black dashed lines and are numbered in the order of their creation.

$U/\sqrt{gh_0}$	F_0	$2\overline{f_s}\sqrt{h_0/g}$	$F_0/(h_1/h_0-1)$	$\overline{St}$
0·90	1·80	0·36	1·64	0·22
0·80	1·66	0·40	1·84	0·22
0·70	1·59	0·51	1·99	0·26
0·60	1·52	0·40	2·17	0·19
0·50	1·37	0·61	2·74	0·22

Table 2: Vortex creation during the splash-up cycles for different piston velocities. $\overline{f_s}$, $\overline{St}$ represent the averaged values for the dimensionless frequency of shedding and for the Strouhal number defined in Eq. [2].

If $N_V(t;t_0)$ is the number of vortical structures generated from when the first plunging jet hits the free surface at t_0 up to the current time t, the frequency of the shedding of vortices with the same sign is

$$f_s(t;t_0) := \frac{N_V(t;t_0)/2}{(t-t_0)} \qquad St := f_s\frac{h_1-h_0}{u} = f_s\sqrt{\frac{h_0}{g}}\Big/\left(\frac{F_0}{h_1/h_0\,-\,1}\right). \tag{2}$$

Taking the ratio $(h_1-h_0)/u$ as the characteristic time scale for the bore evolution we can introduce a Strouhal number as defined in equation (2). Fixing the time interval $[t_0,t]$, as F_0 decreases the size of the vortical structures generated reduces and their number increases. This implies that the averaged value of f_s increases. Also the term $F_0/(h_1/h_0-1)$ increases with the Froude number, almost with the same trend as f_s (see table 2). As a consequence, except for small fluctuations, St remains almost constant and equal to about 0·22.

BORES ON BEACHES

The problem of the run-up of waves on sloping beaches is widely treated because of its practical importance: coastal erosion, flooding, for example. Here we present some results for fully-developed bores climbing up beaches with constant slope α. Again a piston with a constant forward motion is employed. This leaves a fully-developed breaking bore propagating shoreward, through water with decreasing depth, collapsing down after reaching the shoreline, and eventually entering a running-up mode where splashing at the front is not detected anymore. Once the bore collapsed against the shoreline, the vortices already shed are convected forward by the main flow and go beyond the shoreline. The top plot of figure 5 gives the position of twelve fixed sections where the velocity has been analyzed. A beach slope $\alpha = 3^0$ is considered. An example of the velocity profiles measured along such sections is shown in the middle plot of figure 5. On this plot, one sees the bore front propagating along the inclined beach and the vortical structures interacting with the local sea floor soon after they have been created. As a consequence, close to the bottom the velocity profiles are characterized both by large horizontal and vertical velocity gradients. When the bore front reaches the shoreline a high speed tongue of fluid is created and starts to rise along the initially dry beach. At this stage no additional vortical structures are generated. The bottom plot gives the time histories of the sea-floor tangential velocities u_τ at the same locations as in the middle plot. For all the probes, the evolution of the tangential velocities show large fluctuations due to the presence of the vortical structures shed from the breaking bore front. The maximum velocity recorded exceeds the speed of the bore front $u = 1.66\sqrt{gh_0}$.

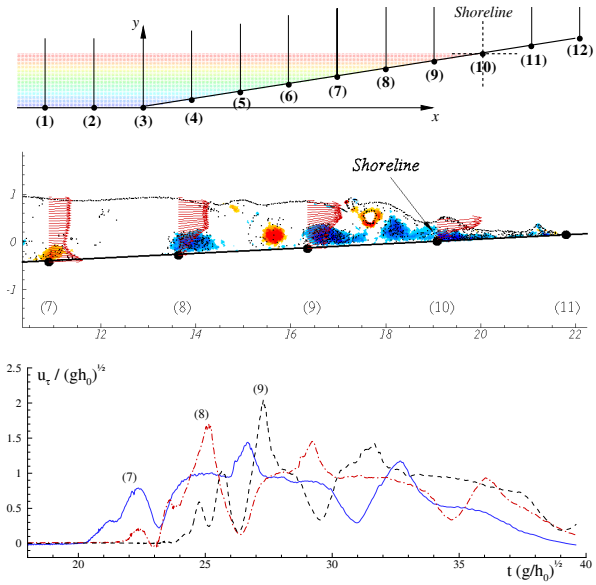

Figure 5: Breaking bore approaching an inclined beach with constant angle α. Top: The black lines indicate the positions of the selected vertical fixed sections where velocities are recorded. Middle: example of velocity profiles and associated vortical structures ($\alpha = 3^0$). Bottom: Time histories of the sea-floor tangential velocities at the same locations.

CONCLUSION

A SPH method is used to achieve long-time simulations of the complex dynamics involved in the cyclical breaking of bores. Splash-up cycles and their link with the genesis of vortical structures downstream the bore are discussed in detail. The presence of vortical structures of opposite sign is detected and connected with the splash-up mechanics. According to the analysis, vortices with opposite sign can pair to form dipole structures. These affect the water evolution and can interact in a complex way with the free surface and with the sea floor. In the latter case, large stresses can be induced at the bottom that are responsible for erosion. The latter phenomenon is quite relevant from practical point of view. Finally, the investigation is extended to the case of breaking bores climbing sloped beaches.

Acknowledgements. This work has been supported at the Ocean Engineering Laboratory, UCSB, as part of a program for the simulation of ship breaking waves by the Ship Hydrodynamics Program of ONR, formerly managed by Dr. Ed Rood and currently by Dr. Pat Purtell. INSEAN research activity is supported by the Italian *Ministero per le Infrastrutture ed i Trasporti* through INSEAN Research Program (Programma Sicurezza) 2003-05.

REFERENCES

[1] R.L. Miller, Role of vortices in surf-zone prediction: sedimentation and wave forces, Soc. Econ. Paleontol. Mineralog. Special Publ. 73 (1976) 92–114.
[2] D.H. Peregrine, Breaking waves on beaches, Ann. Rev. Fluid Mech. 15 (1983) 149–178.
[3] P. Bonmarin, Geometric properties of deep-water breaking waves, J. Fluid Mech. 209 (1989) 405–433.
[4] J.A. Battjes, Surf-zone dynamics, Ann. Rev. Fluid Mech. 20 (1988) 257–293.
[5] P. Wang, Y. Yao & M.P. Tulin, An efficient numerical tank for nonlinear water waves based on the multi-subdomain approach with BEM, Int. J. Numer. Meth. Fluids 20 (1995) 1315–1336.
[6] E.D. Christensen & R. Deigaard, Large eddy simulation of breaking waves, Coastal Engineering 42 (2001) 53–86.
[7] Y. Watanabe & H. Saeki, Velocity fields after wave breaking, Int. J. Numer. Meth. Fluids 39 (2002) 607–637.
[8] J.J. Monaghan, Simulating Free Surface Flows with SPH, J. Comput. Phys. 110 (1994) 399–406.
[9] A. Colagrossi & M. Landrini, Numerical simulation of interfacial flows by Smoothed Particle Hydrodynamics, J. Comput. Phys. 191 (2003) 448–475.
[10] A. Colagrossi, A meshless Lagrangian method for free-surface and interface flows with fragmentation, PhD Thesis, University of Rome La Sapienza (Italy), 2005.
[11] R.L. Miller, Experimental Determination of Run-Up of Undular and Fully Developed Bores, J. Geophys. Res. 73 (1968) 4497–4510.
[12] M. Greco, A two-dimensional study of green-water loading, PhD Thesis, University of Trondheim (Norway), 2001.
[13] G.B. Deane & D.M. Stokes, Scale dependence of bubble creation mechanisms in breaking waves, Nature 418 (2002) 839–844.